molecular pharmaceutics

Article

pubs.acs.org/molecularpharmaceutics

Cetuximab Reduces the Accumulation of Radiolabeled Bevacizumab in Cancer Xenografts without Decreasing VEGF Expression

Sandra Heskamp,*[,†] Otto C. Boerman,[†] Janneke D. M. Molkenboer-Kuenen,[†] Fred C. G. J. Sweep,[‡] Anneke Geurts-Moespot,[‡] Mallory S. Engelhardt,[†] Winette T. A. van der Graaf,[§] Wim J. G. Oyen,[†] and Hanneke W. M. van Laarhoven[§,∥]

[†]Department of Radiology and Nuclear Medicine, [‡]Department of Laboratory Medicine, [§]Department of Medical Oncology, Radboud University Medical Center, P.O. Box 9101, 6500 HB Nijmegen, The Netherlands

[∥]Department of Medical Oncology, Academic Medical Center, University of Amsterdam, Meibergdreef 9, 1105 AZ Amsterdam, The Netherlands

Supporting Information

ABSTRACT: Bevacizumab and cetuximab are approved for the treatment of cancer. However, in advanced colorectal cancer, addition of cetuximab to chemotherapy with bevacizumab did not improve survival. The reason for the lack of activity remains unclear. The aim of this study was to determine the effect of cetuximab on VEGF expression and targeting of bevacizumab to the tumor. Mice with subcutaneous SUM149 or WiDr xenografts were treated with cetuximab, bevacizumab, or a combination of the two. Before the start of cetuximab treatment and after 7 and 21 days of treatment, the uptake of radiolabeled bevacizumab in the tumor was measured by immunoSPECT/CT. Tumor growth of SUM149 xenografts was significantly inhibited by cetuximab, bevacizumab, or their combination, whereas growth of WiDr xenografts was not affected. Cetuximab caused a significant reduction of bevacizumab uptake in SUM149 xenografts, whereas tumor-to-blood ratios in mice with WiDr xenografts did not change. Biodistribution studies with an irrelevant antibody in the SUM149 model also showed significantly reduced tumor-to-blood ratios. Cetuximab treatment did not decrease VEGF expression. Without decreasing VEGF levels, cetuximab reduces tumor targeting of bevacizumab. This could, at least partly, explain why the combination of bevacizumab and cetuximab does not result in improved therapeutic efficacy.

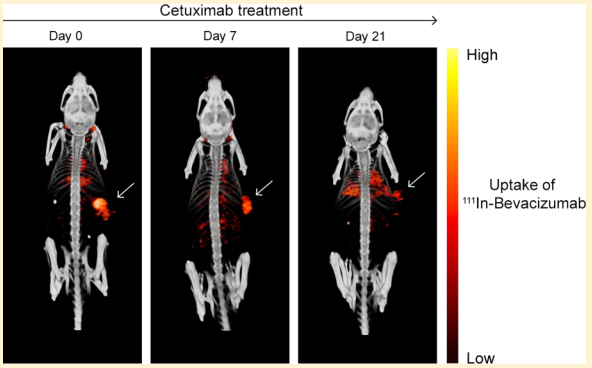

KEYWORDS: *bevacizumab, cetuximab, EGFR, SPECT, VEGF*

INTRODUCTION

Cetuximab is currently approved for treatment of patients with metastatic colorectal cancer and advanced squamous cell carcinoma of the head and neck. It is a chimeric monoclonal antibody that inhibits the epidermal growth factor receptor (EGFR).[1] Although cetuximab in combination with chemotherapy has been shown to improve survival of cancer patients, its therapeutic efficacy is still limited, and ultimately most patients will develop progressive disease.[2,3] Therefore, new therapeutic strategies are being investigated. For example, different antibodies may be combined to improve survival. However, the development of an effective, rational combination remains challenging.

Agents targeting the closely related VEGF and EGFR pathways have potential for combination therapy. In vitro studies have shown a correlation between increased VEGFR-1 expression and resistance to EGFR-targeted therapy.[4] Moreover, in the case of hypoxic conditions, hypoxia-inducible transcription factors (HIFs) are able to upregulate the expression of EGFR.[5] Furthermore, EGFR activation can induce tumor cell VEGF production, causing endothelial cells to proliferate and migrate.[6] In contrast, blocking EGFR can decrease the expression of VEGF.[7]

Early studies have shown that inhibiting both EGFR and angiogenesis may result in enhanced therapeutic efficacy.[8−13] Moreover, the combination of bevacizumab with chemotherapy improves the survival of colorectal cancer patients.[14] Therefore, phase III clinical trials have studied the therapeutic efficacy of the combination of chemotherapy with both cetuximab and bevacizumab or panitumumab and bevacizumab. However, this did not improve the progression-free survival compared with that of patients who were treated with bevacizumab and chemotherapy alone.[15−17]

There are several potential explanations for this observation. For example, dual-pathway targeting with panitumumab and

Received: July 2, 2014
Revised: October 7, 2014
Accepted: October 8, 2014
Published: October 8, 2014

bevacizumab may have caused enhanced toxicity, leading to dose reductions or dose delays,[17] although this was not observed in other studies.[15] Also, pharmacokinetic interactions might have occurred between the antibodies, as was suggested by a decrease in the incidence of bevacizumab-induced hypertension in the group receiving both bevacizumab and cetuximab.[17] Furthermore, we have shown that bevacizumab alters tumor vascularity of subcutaneous human xenografts in mice, thereby limiting the delivery of cetuximab to the tumor. This can lead to reduced therapeutic efficacy.[18] Finally, interactions may have occurred between the downstream signaling pathways. For example, EGFR-mediated changes in downstream targets may be necessary for the antitumor activity of bevacizumab or chemotherapy.[17]

In this study, we determined whether cetuximab treatment has an effect on VEGF expression and the accumulation of bevacizumab in the tumor. For that purpose, mice with subcutaneous VEGF and EGFR-expressing tumors were treated with cetuximab, and we measured the effect on tumor targeting of radiolabeled bevacizumab with SPECT/CT and analyzed the tumors for VEGF expression.

MATERIAL AND METHODS

Cell Culture and Antibodies. The breast cancer cell line SUM149 (Asterand, Detroit, MI) was cultured in Ham's F12 medium (GIBCO, BRL Life Sciences Technologies, The Netherlands) supplemented with 5% fetal calf serum (FCS), 10 mM 4-(2-hydroxyethyl)-1-piperazineethanesulfonic acid (HEPES), hydrocortisone (1 μg/mL), and insulin (5 μg/mL) at 37 °C in a humidified atmosphere with 5% CO_2. The colorectal cancer cell line WiDr was cultured in DMEM with 1000 mg/L D-glucose/Ham's F12 medium (1:1 mixture) supplemented with 2 mM glutamine and 10% FCS.

Cetuximab, a chimeric monoclonal antibody directed against human EGFR, was obtained from Merck (Darmstadt, Germany). Bevacizumab, a humanized monoclonal antibody against VEGF, was obtained from Roche (Basel, Switzerland). The humanized anti-CD22 antibody hLL2 was kindly supplied by Immunomedics, Inc. (Morris Plains, NJ, USA) and was used as an irrelevant control antibody in this study.

Radiolabeling. Bevacizumab and hLL2 (10 mg/mL) were conjugated with isothiocyanatobenzyl-diethylenetriaminepentaacetic acid (ITC-DTPA, Macrocyclis, Dallas, TX) in 0.1 M $NaHCO_3$, pH 9.5, at a 15-fold molar excess of ITC-DTPA for 1 h at room temperature (RT). The unbound ITC-DTPA was removed from the reaction mixture by dialysis against 0.25 M ammonium acetate buffer, pH 5.4. DTPA-conjugated antibodies (10−20 μg) were incubated with (110−220 MBq) ^{111}In (Covidien BV, Petten, The Netherlands) in 0.1 M 2-(*N*-morpholino)ethanesulfonic acid (MES) buffer, pH 5.4, at room temperature (RT) under strict metal-free conditions for 30 min.[19] After incubation, 50 mM ethylenediaminetetraacetic acid (EDTA) was added to a final concentration of 5 mM to chelate unincorporated ^{111}In. Labeling efficiency was determined using instant thin-layer chromatography (ITLC) on silica gel chromatography strips (Agilent Technologies, Palo Alto, CA) using 0.1 M citrate buffer, pH 6.0, as the mobile phase. In cases where the labeling efficiency was below 95%, the reaction mixture was purified on a PD-10 column (Amersham Biosciences, Uppsala, Sweden) and eluted with PBS containing 0.5% BSA. The radiochemical purity of ^{111}In-DTPA-bevacizumab (^{111}In-Bevacizumab) and ^{111}In-DTPA-hLL2 (^{111}In-hLL2) exceeded 95% in all experiments.

In Vitro Experiments. *EGFR and CD22 Expression of SUM149 and WiDr Cells.* Scatchard analysis was performed to quantitatively determine EGFR expression of SUM149 and WiDr cells. Cells were cultured to confluency in six-well plates and were incubated for 4 h on ice with increasing concentrations of ^{111}In-cetuximab (0.03−300 nM) in 1 mL of binding buffer (Ham's F12 containing 10 mM HEPES and 0.5% bovine serum albumin (BSA)). The cell-associated activity at each concentration was determined in triplicate. Nonspecific binding was determined by coincubation with 3 μM cetuximab. After incubation, cells were washed with PBS, and the cell-associated activity was measured in a shielded well-type gamma counter (PerkinElmer, Boston, MA, USA). The specific binding was plotted against the bound/free ratio, and data were analyzed by linear regression to determine EGFR receptor density per cell and to determine the dissociation constant (K_d) of ^{111}In-cetuximab.

The anti-CD22 antibody hLL2 (IgG1) was used as a control antibody without specific tumor targeting. To confirm that the SUM149 and WiDr cell lines do not express CD22, cells were incubated with 0.3 nM ^{111}In-hLL2. Separate wells were coincubated with an excess of unlabeled hLL2 (30 nM). After 4 h on ice, cells were washed, and cell-associated activity was measured as described above.

MTT Assays. The effect of cetuximab on cell viability was assessed in an MTT assay. SUM149 or WiDr cells (5000 cells/well) were allowed to adhere overnight in a 96-well plate. Subsequently, cells were incubated with cetuximab (0.1−6000 nM) for 72 h at 37 °C in a humidified atmosphere with 5% CO_2. After incubation, MTT (final concentration 0.5 mg/mL) was added and incubated for 3.5 h at 37 °C, followed by 15 min incubation with MTT solvent (isopropanol containing 4 mM HCl, 0.1% NP-40) at RT. Absorbance was read at 560 and 655 nm. IC_{50} values were calculated with GraphPad Prism, version 5.03.

In Vitro Effect of Cetuximab on VEGF Expression. SUM149 and WiDr cells were cultured in the presence of 1, 10, or 100 nM cetuximab. Before treatment and 1, 4, and 7 days after the start of treatment, cells were trypsinized, washed, and lysed using T-per tissue protein extract (no. 78510, Thermo Scientific, Etten Leur, The Netherlands) followed by sonification. Cell extracts were diluted 5×, and VEGF levels were determined with ELISA as described below.

Animal Experiments. Animal experiments were performed in female BALB/c nude mice (Janvier, le Genest-Saint-Isle, France) and were conducted in accordance with the principles laid out by the revised Dutch Act on Animal Experimentation (1997) and approved by the Institutional Animal Welfare Committee of the Radboud University Nijmegen. At 6−8 weeks of age, mice were inoculated subcutaneously with 5×10^6 SUM149 (in 0.2 mL of 2:1 Ham's F12 medium/matrigel, BD Biosciences, Pharmingen) or 5×10^6 WiDr cells (in 0.2 mL of 1:1 Ham's F12/DMEM medium). Experiments started when the tumors reached a size of approximately 0.1 cm^3.

Effect of Cetuximab, Bevacizumab, and Their Combination on Tumor Growth. Mice with s.c. SUM149 or WiDr tumors (n = 6 per group) were injected intraperitoneally, twice a week, with cetuximab (SUM149, 1 mg/kg; WiDr, 40 mg/kg), bevacizumab (10 mg/kg), or a combination of these agents (using the same dosage as in the monotherapy groups). To be able to compare the results from the therapy studies with those from the imaging studies, in the combined treatment group, cetuximab treatment started at day 0 and bevacizumab

treatment at day 4. The cetuximab dose was based on previous dose optimization studies performed in the SUM149 model. Tumor growth of SUM149 xenografts was significantly inhibited by cetuximab in a dose-independent manner (range 1−40 mg/kg, Supporting Information Figure 1). Since WiDr xenografts are much less sensitive to cetuximab, a higher cetuximab dose of 40 mg/kg was chosen.[20] Tumor size was measured three times a week by caliper measurements in three dimensions (radius x, y, and z). Tumor size was calculated using the following formula: $^4/_3\pi xyz$. Body weight was measured three times a week. EDTA blood samples were collected weekly from mice that were treated with cetuximab alone to determine the plasma levels of cetuximab by ELISA. Samples were centrifuged for 10 min at 1600g, and plasma was stored at −80 °C until further analysis.

Effect of Cetuximab on VEGF Expression and Targeting of Radiolabeled Bevacizumab. Mice with s.c. SUM149 or WiDr tumors (n = 5 per group) were injected intraperitoneally, twice a week, with cetuximab (SUM149, 1 mg/kg; WiDr, 40 mg/kg) or vehicle. The effect of cetuximab treatment on targeting of ^{111}In-bevacizumab and ^{111}In-hLL2 to SUM149 and WiDr xenografts was measured by ex vivo biodistribution and SPECT/CT. Before the start of treatment (day −3) and at days 4 and 18 of treatment, mice were injected with ^{111}In-bevacizumab. Three days later (days 0, 7, and 21), mice were euthanized, and tumor, blood, muscle, lung, spleen, pancreas, intestine, kidney, and liver were dissected and weighed. Activity was measured in a gamma counter. To calculate the uptake of radiolabeled antibodies in each sample as a fraction of the injected dose, aliquots of the injected dose were counted simultaneously. The concentrations of the radiolabeled antibody were expressed as percentage injected dose per gram of tissue (%ID/g). Tumor samples were fixed in 4% formalin or frozen at −80 °C to analyze VEGF expression by immunohistochemistry and ELISA. EDTA blood samples were collected and centrifuged for 10 min at 1600g, and plasma was stored at −80 °C until further analysis of VEGF levels.

Separate mice were used for SPECT/CT imaging. Three days prior to SPECT/CT acquisition, mice were injected intravenously with 2.4 μg (SUM149) or 2.0 μg (WiDr) of ^{111}In-bevacizumab (20−30 MBq). SPECT/CT images were acquired at days 0, 7, and 21 using the U-SPECT-II/CT system (MILabs, Utrecht, The Netherlands).[21] Mice were scanned for 50 min using the 1.0 mm diameter pinhole mouse high-sensitivity collimator tube, followed by a CT scan (spatial resolution 160 μm, 65 kV, 612 μA) for anatomical reference. Scans were reconstructed with MILabs reconstruction software, which uses an ordered-subset expectation maximization algorithm, with a voxel size of 0.2 mm.

Immunohistochemistry. Antibodies against EGFR (D38B1 Cell Signaling), CD34 (MON1159, clone MEC14.7, Monosan), and VEGF (555036, Pharmingen) were used to determine expression of the respective antigens on paraffin-embedded tumor sections. In short, antigen retrieval was performed in 10 mM sodium citrate, pH 6.0, for 10 min at 99 °C for EGFR and CD34 staining. Endogenous peroxidase activity was blocked with 3% H_2O_2, and nonspecific binding was blocked by incubation with normal goat serum. After incubation with the primary antibody, tumor sections were incubated with a biotinylated secondary antibody, followed by incubation with an avidin−biotin−enzyme complex (Vector Laboratories, Burlingame, CA). Finally, 3,3′-diaminobenzidine (DAB) was used to develop the staining of the tumor sections.

EGFR expression was scored as negative (0: no staining is observed, or membrane staining is observed in <10% of the tumor cells), incomplete weak (1+: a faint/barely perceptible membrane staining is detected in >10% of tumor cells; the cells exhibit incomplete membrane staining), complete weak to moderate (2+: a weak to moderate complete membrane staining is observed in >10% of tumor cells), and strong (3+: a strong complete membrane staining is observed in >10% of tumor cells) membrane staining. The mean vascular density (MVD) was scored as the number of vessels counted in 3 hot spot areas that contained the maximum number of vessels.

ELISA VEGF Levels. VEGF levels in plasma and tumor tissue was determined with ELISA. Frozen tumors were pulverized with liquid nitrogen using a microdismembrator in EORTC buffer (20 mmol/L K_2HPO_4/KH_2PO_4, 1.5 mmol/L K_2EDTA, 3 mmol/L sodium azide, 10 mmol/L monothioglycerol, 10% [v/v] glycerol/water, pH 7.4) and centrifuged at 105 000g. The protein concentration of the cell lysates and tumor lysates was measured using a Pierce BCA assay kit (no. 23227, Pierce, Rockford, IL). Antigen levels of VEGF in cell extracts, plasma, and tumor extracts were measured by a specific ELISA as described by Span et al.[22] The assay applies a combination of four polyclonal antibodies (raised in four different animal species) employed in a sandwich assay format to exclude heterophilic antibody interference.[23] To increase the sensitivity of the VEGF assay, the HRP-labeled goat anti-rabbit detection antibody was replaced by a goat anti-rabbit IgG biotin conjugate (no. B-9642, Sigma Chemical Co, St. Louis, MO), streptavidin-labeled β-galactosidase (no. 1112481, Boehringer Mannheim, Germany) was used as enzyme, and 4-methyl-umbelliferyl-β-D-galactopyranoside (MUG, Sigma Chemical, St. Louis, MO) was used as substrate. In this assay, distinct molecular forms of VEGF, such as VEGF-165 and VEGF-121, are measured. No cross-reactivity could be demonstrated with several other growth factors. The analytical sensitivity of the VEGF assay is 0.005 ng/mL. The within-assay and between-assay coefficients of variation were 8.7 and 13.4%, respectively.

ELISA Cetuximab Levels. To determine plasma cetuximab levels, an ELISA was performed as described previously.[24] Plates were coated with a recombinant form of EGFR (human Sf9, Genway, San Diego, CA 92121, USA, 0.1 μg/well) in 15 mmol/L Na_2CO_3 and 35 mmol/L $NaHCO_3$, pH 9.6. After blocking (1% BSA in PBS), plasma samples (diluted 1600× in BSA/PBS/Tween-20) and reference samples (cetuximab, range 0−32 ng/mL) were incubated overnight at 4 °C. Subsequently, plates were incubated with mouse anti-human IgG (Fc) HRP (SouthernBiotech, Birmingham, U.K., dilution 1:25 000), followed by incubation with TMB solution (Kem-En-Tec, Taastrup, Denmark). The reaction was stopped by addition of 100 μL of 0.5 M H_2SO_4, and optical density was measured at 450 nm. Imprecision and accuracy of calibrators and samples were 10% or less. The lower limit of detection was 0.09 ng/L.

Statistical Analysis. Statistical analyses were performed using PASW Statistics, version 18.0 (Chicago, IL), and GraphPad Prism, version 5.03 (San Diego, CA), for Windows. Differences in tumor size and uptake of radiolabeled antibodies before and after cetuximab treatment were tested for significance using the nonparametric Kruskal−Wallis and Mann−Whitney U test. A p-value below 0.05 was considered significant.

RESULTS

In Vitro Experiments. Scatchard analysis showed that the receptor density of EGFR was 108 100 receptors/cell (95% CI, 88 400−142 000 receptors/cell) and 21 100 receptors/cell (95% CI, 17 100−28 100 receptors/cell) for SUM149 and WiDr cells, respectively. The K_d of ^{111}In-cetuximab determined on SUM149 cells was 0.21 nM (95% CI, 0.16−0.28 nM). The irrelevant IgG ^{111}In-hLL2 did not show specific binding on SUM149 or WiDr cells.

The growth of the SUM149 cells was inhibited by cetuximab: The IC_{50} value for SUM149 was 6.0 nM (95% CI, 2.7−13.5 nM). WiDr cells were less sensitive to cetuximab treatment (IC_{50} > 1 μM) (Figure 1A). In vitro, cetuximab dose-dependently seemed to decrease the expression of VEGF in SUM149 cells, whereas the expression in WiDr cells did not seem change (Figure 1B,C).

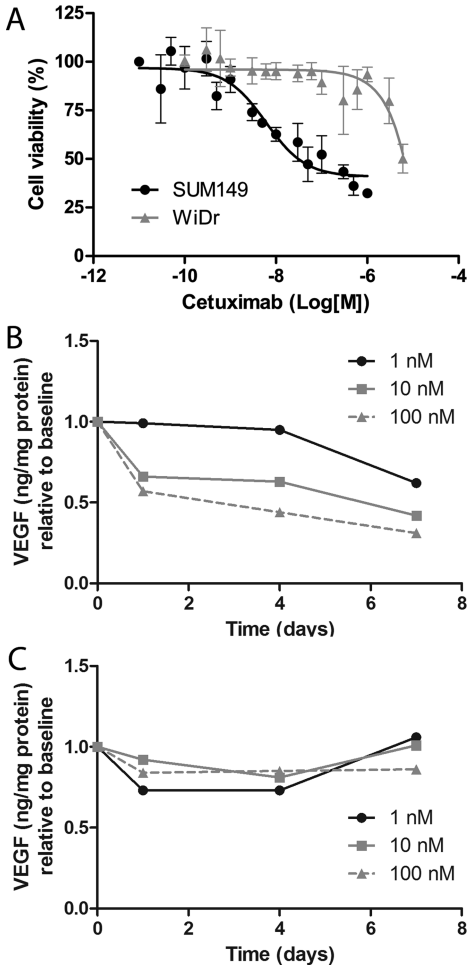

Figure 1. (A) Cell viability of SUM149 and WiDr cells after a 72 h incubation with cetuximab. The IC_{50} value of cetuximab for SUM149 cells was 6.0 nM (95% CI, 2.7−13.5 nM). The IC_{50} for WiDr cells could not be reliable estimated. (B) VEGF expression of SUM149 and (C) WiDr cells during cetuximab treatment in vitro.

Animal Experiments. *Effect of Cetuximab, Bevacizumab, and the Combination on Tumor Growth.* Plasma levels of cetuximab gradually increased over time and reached a plateau after 21 days of treatment (Figure 2A). Cetuximab, bevacizumab, and the combination of these two agents significantly inhibited growth of the SUM149 tumors. Tumor

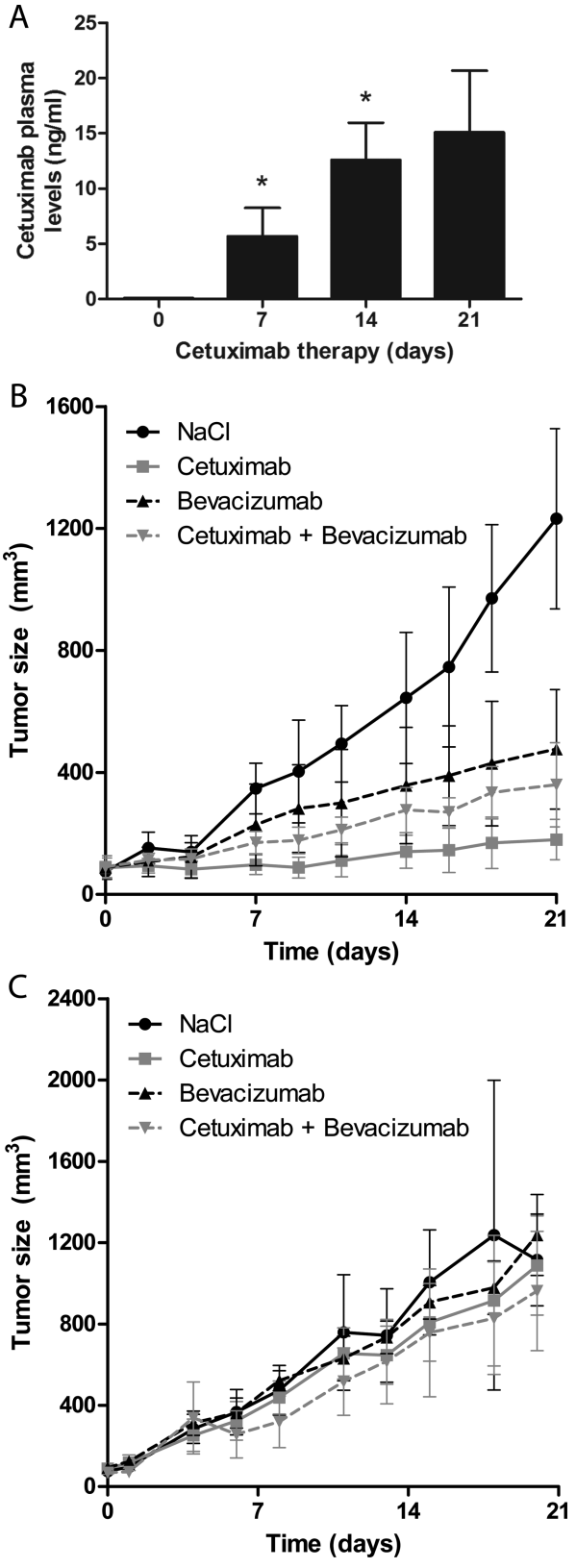

Figure 2. (A) Cetuximab plasma levels of mice bearing subcutaneous SUM149 xenografts treated once per week intraperitoneally (1 mg/kg). Asterisks (*) indicate a significant increase in cetuximab concentration compared to that at the previous time point. (B) Tumor growth of SUM149 and (C) WiDr xenografts during treatment.

size at day 21 was significantly less for treated tumors compared to that of untreated tumors ($p < 0.001$, Figure 2B,C). Furthermore, tumor growth was more effectively inhibited by cetuximab alone compared to that with either bevacizumab alone ($p = 0.017$) or the combination of cetuximab and bevacizumab ($p = 0.032$). In the WiDr model, tumor growth was not significantly inhibited by cetuximab, bevacizumab, or the combination therapy.

Tumor Targeting of ^{111}In-Bevacizumab and ^{111}In-hLL2. The tumor targeting of ^{111}In-bevacizumab was significantly reduced in cetuximab-treated SUM149 tumors compared to that in untreated tumors. Tumor uptake at day 0 (before treatment) and at days 7 and day 21 after treatment, as measured in the ex vivo biodistribution study, was 28.9 ± 4.0, 21.9 ± 1.7, and 18.2 ± 2.8%ID/g, respectively ($p = 0.003$). Tumor-to-blood ratios at these time points were 2.4 ± 0.3, 1.6 ± 0.2, and 1.4 ± 0.2, respectively ($p = 0.004$, Figure 3). SPECT/CT imaging showed that tumor targeting of ^{111}In-bevacizumab was clearly reduced after cetuximab treatment of mice with subcutaneous SUM149 tumors (Figure 4).

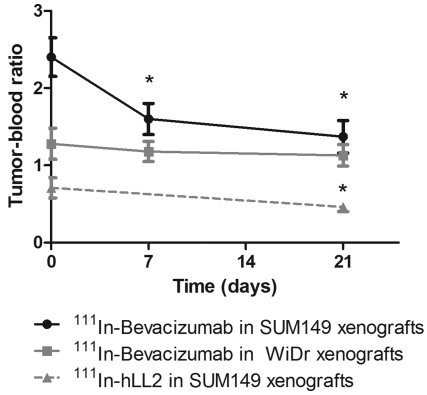

Figure 3. Tumor blood ratios of mice with subcutaneous SUM149 and WiDr xenografts before and during cetuximab treatment (3 days p.i., 1 μg ^{111}In-bevacizumab or ^{111}In-hLL2). Asterisks (*) indicate a significant change compared to the tumor−blood ratio at day 0.

SPECT/CT imaging of cetuximab treated mice with subcutaneous WiDr xenografts showed no effect on the biodistribution of ^{111}In-bevacizumab at day 7 of treatment, whereas at day 21, tumor uptake and blood levels of ^{111}In-bevacizumab were significantly decreased. Tumor uptake at days 0, 7, and 21 was 17.3 ± 2.4, 14.2 ± 1.0, and 9.9 ± 1.7%ID/g, respectively (day 21 versus day 0, $p = 0.008$). Tumor-to-blood ratios at these days were 1.3 ± 0.2, 1.2 ± 0.1, and 1.1 ± 0.1, respectively, and did not differ significantly.

To study whether the effect of cetuximab on bevacizumab targeting was specific for VEGF or whether other features of the tumor (e.g., vascularization, vascular permeability, interstitial fluid pressure, etc.) were also involved, we determined the biodistribution of an irrelevant control antibody (hLL2) in SUM149 tumors. At day 21 of cetuximab treatment, tumor uptake and tumor-to-blood ratios of ^{111}In-hLL2 decreased significantly compared to those at day 0 (tumor uptake, 8.2 ± 2.2%ID/g versus 4.6 ± 0.6%ID/g ($p = 0.016$); tumor-blood ratio, 0.7 ± 0.1 versus 0.5 ± 0.1 ($p = 0.016$)), suggesting that cetuximab affects tumor physiological factor such as vascular permeability and/or interstitial fluid pressure.

To exclude the possibility that the changes in tumor targeting were caused by other tumor factors that changed during tumor progression rather than cetuximab alone, we included a control group at days 7 and 21 that received saline only. In the ex vivo biodistribution, tumor uptake before treatment and after 7 and 21 days of cetuximab treatment was 24.9 ± 3.1, 28.0 ± 3.4, and 24.9 ± 0.8%ID/g, respectively. The tumor uptake of saline-treated mice at days 7 and 21 was 30.6 ± 2.9 and 35.1 ± 7.2% ID/g, which is significantly higher compared to that for the cetuximab-treated mice. For WiDr tumors treated with cetuximab, tumor uptake at days 0, 7, and 21 was 16.1 ± 0.6, 21.5 ± 2.5, and 13.1 ± 2.1%ID/g, respectively. Mice that were treated with saline showed a similar tumor uptake of 23.8 ± 2.0 and 12.1 ± 1.7%ID/g at days 7 and 21, respectively.

Immunohistochemistry. The viability of the tumor was checked by H&E staining. SUM149 xenografts (both treated and untreated) consisted of >80% viable tumor tissue. For WiDr, we observed a small decrease in the viable tumor fraction at day 21 of treatment. Necrotic areas developed, most likely due to the very rapid growth of these xenografts.

EGFR immunostaining showed that cetuximab treatment resulted in decreased expression of EGFR. Untreated SUM149 xenografts were scored 3+, whereas 21 days of cetuximab

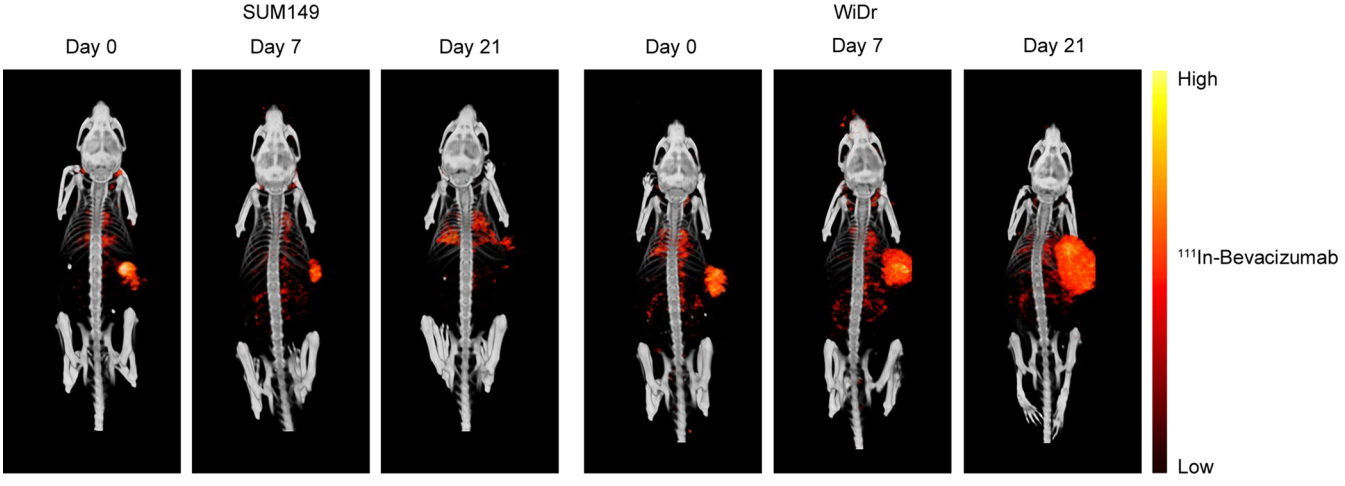

Figure 4. SPECT/CT scans of mice with subcutaneous SUM149 and WiDr xenografts before and during cetuximab treatment (3 days p.i., 2.4−3 μg ^{111}In-bevacizumab).

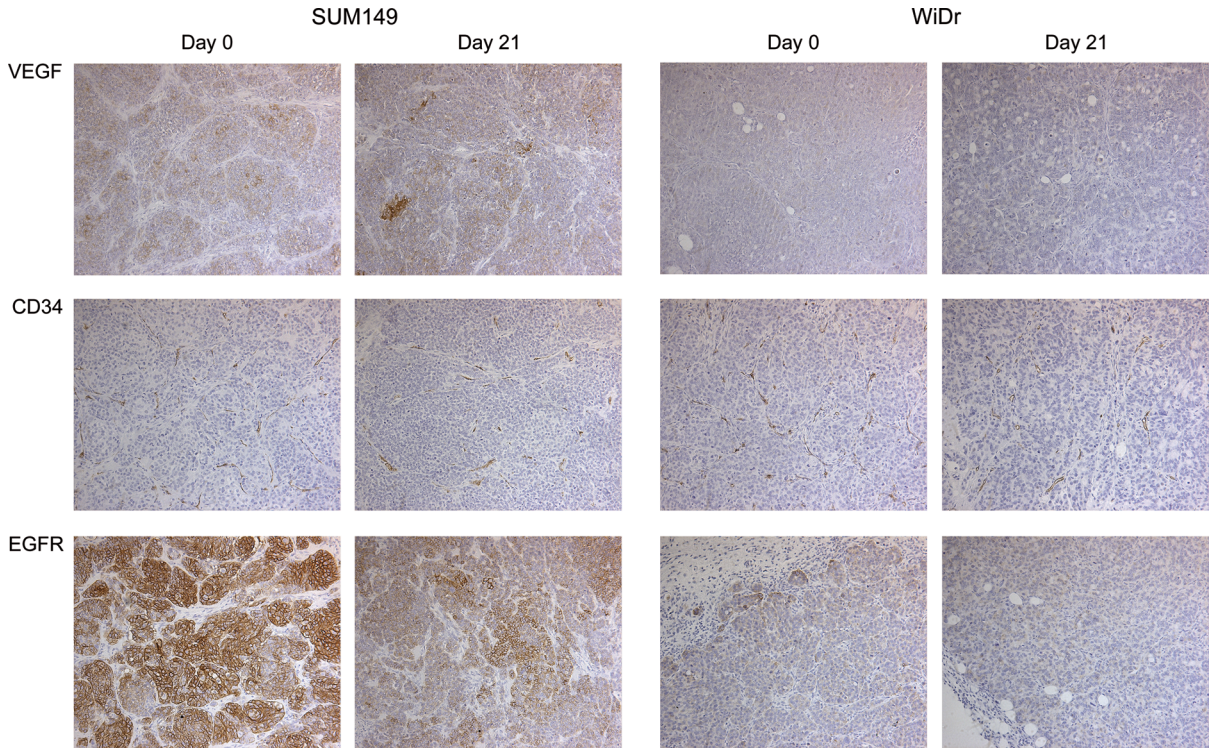

Figure 5. Immunohistochemical analysis of SUM149 and WiDr xenografts. Magnification 200× (VEGF and CD34) and 400× (EGFR).

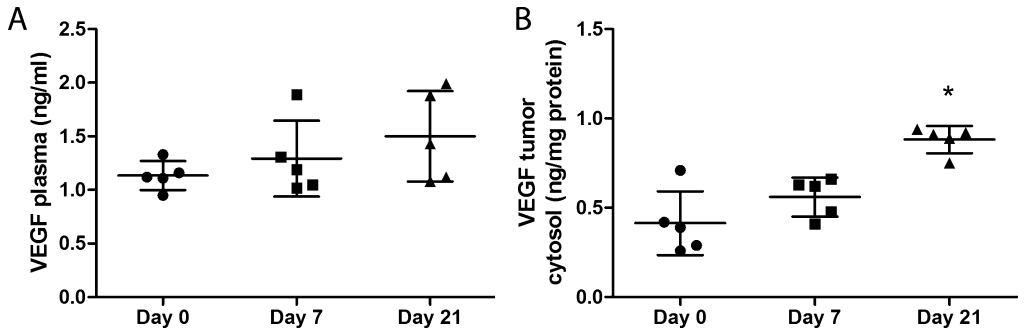

Figure 6. VEGF levels in plasma (A) and SUM149 tumors (B) of cetuximab-treated mice.

treatment resulted in a score of 2+. For WiDr, EGFR expression before and after treatment was 2+ and 1+, respectively. The microvascular density (CD34) was not significantly reduced during cetuximab treatment (Figure 5).

Immunohistochemical analysis of VEGF expression did not show a clear reduction, whereas some isolated fields of cells showed increased VEGF expression. Further examination of these areas with high VEGF expression with H&E and Ki67 staining showed that these cells were morphologically different from the tumor cells. These cells were larger and contained relatively more cytoplasm compared to that of the surrounding small tumor cells. In addition, these cells were Ki67 negative, whereas the surrounding cells were Ki67 positive. This suggests that these fields with high VEGF expressing cells may contain differentiated tumor cells.

ELISA. Analysis of plasma and tumor VEGF levels with ELISA showed that plasma VEGF did not change during cetuximab treatment. Tumor VEGF levels were significantly increased after 21 days of cetuximab treatment (Figure 6).

DISCUSSION

This study shows that cetuximab can significantly hamper the targeting of bevacizumab to a tumor. This is most likely caused by a change in tumor physiology, such as vascular permeability and intratumoral interstitial fluid pressure, since the tumor targeting of the irrelevant control antibody was also significantly reduced and no clear decrease in VEGF expression was observed.

Previous studies have shown extensive crosstalk between EGFR and VEGF, providing a rational to combine anti-EGFR and anti-VEGF treatments. However, phase III clinical studies have shown that the combination of cetuximab with chemotherapy and bevacizumab did not result in improved survival of colorectal cancer patients.[15−17] This was unexpected, since early preclinical studies have shown encouraging results for the combination of agents that target angiogenesis and EGFR.[8−11] However, these studies did not assess the combination of cetuximab and bevacizumab. More recently, the combination of these two agents was studied by Wang et al. They showed that the growth inhibition of head and neck squamous cell carcinoma xenografts was less effective after treatment with

the triple agent combination (cetuximab, bevacizumab, and cisplatin) compared with that using bevacizumab and cisplatin alone.[25] Moreover, Poindessous et al. showed that the combined treatment (cetuximab and bevacizumab) of colon cancer xenografts was equally effective as that with either agent alone.[26] This is in line with the findings in our study that the combination of bevacizumab and cetuximab does not increase therapeutic efficacy compared with that using bevacizumab or cetuximab alone.

Several explanations have been proposed for the lack of an additive effect of the combined treatment with cetuximab and bevacizumab. Previously, we and others have shown that bevacizumab can reduce the vascular density of the tumor and that this could reduce effective targeting of other monoclonal antibodies, such as trastuzumab, R1507 (anti-IGF-1R), and cetuximab, to the tumor.[18,27,28] In this study, we have shown that cetuximab can also hamper the delivery of bevacizumab to the tumor. One potential explanation for this reduced targeting is that cetuximab treatment decreases VEGF expression. Although previous studies showed that blocking of EGFR decreases VEGF protein and mRNA expression,[7,29,30] we did not observe this in our study. Immunohistochemical analysis of tumor sections showed that, overall, the VEGF expression was not altered during cetuximab treatment. There were even some fields of cells showing increased VEGF expression. Also, ELISA did not show a decrease in VEGF levels in the cetuximab-treated mice. In fact, an increase in VEGF expression was measured with ELISA at day 21, which might be explained by the presence of small fields of differentiated tumor cells that express high levels of VEGF.

Studies with the irrelevant control antibody hLL2 also showed significantly reduced tumor targeting, which suggests that tumor physiological factors may play a role in the reduced targeting of ^{111}In-bevacizumab. In order to determine whether the vascular density was altered during cetuximab treatment, we analyzed CD34 expression of the vessels in the tumors. Previous research has shown that treatment with anti-EGFR antibodies can reduce the microvascular density,[29,30] indicating that EGFR blocking can alter tumor vascularity. In our study, vascular density did not change upon cetuximab treatment. However, other factors, such as interstitial tumor pressure and vascular permeability, also determine the accumulation of antibodies in tumors. These factors may have been altered during therapy, and future research is warranted to investigate their precise role.

The decrease in bevacizumab targeting was observed not only in the cetuximab-responsive SUM149 model but also in the resistant WiDr model. This is most likely due to the very rapid tumor growth of these xenografts (increase of almost 10-fold at day 21 compared to baseline). It has been shown previously that the uptake of radiolabeled antibodies is inversely related with tumor size. In general, larger tumors often show lower antibody uptake in terms of the percent injected dose per gram of tissue.[31,32]

Reduced delivery of bevacizumab to the tumor may result in less effective tumor growth inhibition. Therefore, it is important to carefully evaluate the sequencing and timing of antibody treatment. A possible limitation of our studies is that tumor growth and angiogenesis is typically more rapid in preclinical models compared with that in human tumors. Also, murine tumor vessels in xenograft models are more responsive to antiangiogenic therapy compared with that for human tumor vessels.[33] To our knowledge, no clinical studies have shown that tumor VEGF expression and targeting of bevacizumab to the tumor is altered during cetuximab therapy.

CONCLUSIONS

Our study shows that cetuximab significantly hampers the tumor targeting of bevacizumab, whereas no correlation was found between bevacizumab uptake and VEGF expression level. The reduced targeting of bevacizumab can potentially result in reduced therapeutic efficacy. Future studies need to assess how the sequencing and timing of cetuximab in combination with other targeted therapies is related to tumor targeting and tumor growth inhibition.

ASSOCIATED CONTENT

Supporting Information

Tumor growth of subcutaneous SUM149 xenografts, treated with different dosis cetuximab. This material is available free of charge via the Internet at http://pubs.acs.org.

AUTHOR INFORMATION

Corresponding Author

*Phone: +31-24-36-19097. Fax: +31-24-36-18942. E-mail: sandra.heskamp@radboudumc.nl.

Notes

The authors declare no competing financial interest.

ACKNOWLEDGMENTS

This study was financially supported by a personal research grant of the Dutch Research Council to Hanneke van Laarhoven (016.096.010). We thank Bianca Lemmers-van de Weem, Henk Arnts, Iris Lamers-Elemans, and Kitty Lemmens-Hermans for technical assistance.

ABBREVATIONS

%ID/g, percent injected dose per gram of tissue; ^{111}In, indium-111; BSA, bovine serum albumin; DAB, 3,3′-diaminobenzidine; EDTA, ethylenediaminetetraacetic acid; EGFR, epidermal growth factor receptor; ELISA, enzyme-linked immunosorbent assay; HEPES, 4-(2-hydroxyethyl)-1-piperazineethanesulfonic acid; HER2, human epidermal growth factor receptor 2; HER3, human epidermal growth factor receptor 3; HIF, hypoxia-inducible transcription factors; IC_{50}, inhibitory concentration 50%; IGF-1R, insulin-like growth factor 1 receptor; ITC-DTPA, isothiocyanatobenzyl-diethylenetriaminepentaacetic acid; ITLC, instant thin-layer chromatography; K_d, dissociation constant; MBq, megabecquerel; MES, 2-(*N*-morpholino)-ethanesulfonic acid; MUG, 4-methylumbelliferyl-β-D-galacto-pyranoside; MVD, mean vascular density; RT, room temperature; SPECT, single photon emission computed tomography; VEGF, vascular endothelial growth factor

REFERENCES

(1) Hynes, N. E.; Lane, H. A. ERBB receptors and cancer: the complexity of targeted inhibitors. *Nat. Rev. Cancer* **2005**, *5*, 341−354.

(2) Cunningham, D.; Humblet, Y.; Siena, S.; Khayat, D.; Bleiberg, H.; Santoro, A.; Bets, D.; Mueser, M.; Harstrick, A.; Verslype, C.; Chau, I.; Van Cutsem, E. Cetuximab monotherapy and cetuximab plus irinotecan in irinotecan-refractory metastatic colorectal cancer. *N. Engl. J. Med.* **2004**, *351*, 337−345.

(3) Jonker, D. J.; O'Callaghan, C. J.; Karapetis, C. S.; Zalcberg, J. R.; Tu, D.; Au, H. J.; Berry, S. R.; Krahn, M.; Price, T.; Simes, R. J.; Tebbutt, N. C.; van Hazel, G.; Wierzbicki, R.; Langer, C.; Moore, M. J.

Cetuximab for the treatment of colorectal cancer. *N. Engl. J. Med.* **2007**, *357*, 2040−2048.
(4) Bianco, R.; Rosa, R.; Damiano, V.; Daniele, G.; Gelardi, T.; Garofalo, S.; Tarallo, V.; De Falco, S.; Melisi, D.; Benelli, R.; Albini, A.; Ryan, A.; Ciardiello, F.; Tortora, G. Vascular endothelial growth factor receptor-1 contributes to resistance to anti-epidermal growth factor receptor drugs in human cancer cells. *Clin. Cancer Res.* **2008**, *14*, 5069−5080.
(5) Franovic, A.; Gunaratnam, L.; Smith, K.; Robert, I.; Patten, D.; Lee, S. Translational up-regulation of the EGFR by tumor hypoxia provides a nonmutational explanation for its overexpression in human cancer. *Proc. Natl. Acad. Sci. U.S.A.* **2007**, *104*, 13092−13097.
(6) Goldman, C. K.; Kim, J.; Wong, W. L.; King, V.; Brock, T.; Gillespie, G. Y. Epidermal growth factor stimulates vascular endothelial growth factor production by human malignant glioma cells: a model of glioblastoma multiforme pathophysiology. *Mol. Biol. Cell* **1993**, *4*, 121−133.
(7) Petit, A. M.; Rak, J.; Hung, M. C.; Rockwell, P.; Goldstein, N.; Fendly, B.; Kerbel, R. S. Neutralizing antibodies against epidermal growth factor and ErbB-2/neu receptor tyrosine kinases down-regulate vascular endothelial growth factor production by tumor cells in vitro and in vivo: angiogenic implications for signal transduction therapy of solid tumors. *Am. J. Pathol.* **1997**, *151*, 1523−1530.
(8) Ciardiello, F.; Bianco, R.; Damiano, V.; Fontanini, G.; Caputo, R.; Pomatico, G.; De Placido, S.; Bianco, A. R.; Mendelsohn, J.; Tortora, G. Antiangiogenic and antitumor activity of anti-epidermal growth factor receptor C225 monoclonal antibody in combination with vascular endothelial growth factor antisense oligonucleotide in human GEO colon cancer cells. *Clin. Cancer Res.* **2000**, *6*, 3739−3747.
(9) Jung, Y. D.; Mansfield, P. F.; Akagi, M.; Takeda, A.; Liu, W.; Bucana, C. D.; Hicklin, D. J.; Ellis, L. M. Effects of combination anti-vascular endothelial growth factor receptor and anti-epidermal growth factor receptor therapies on the growth of gastric cancer in a nude mouse model. *Eur. J. Cancer* **2002**, *38*, 1133−1140.
(10) Shaheen, R. M.; Ahmad, S. A.; Liu, W.; Reinmuth, N.; Jung, Y. D.; Tseng, W. W.; Drazan, K. E.; Bucana, C. D.; Hicklin, D. J.; Ellis, L. M. Inhibited growth of colon cancer carcinomatosis by antibodies to vascular endothelial and epidermal growth factor receptors. *Br. J. Cancer* **2001**, *85*, 584−589.
(11) Tonra, J. R.; Deevi, D. S.; Corcoran, E.; Li, H.; Wang, S.; Carrick, F. E.; Hicklin, D. J. Synergistic antitumor effects of combined epidermal growth factor receptor and vascular endothelial growth factor receptor-2 targeted therapy. *Clin. Cancer Res.* **2006**, *12*, 2197−2207.
(12) Herbst, R. S.; Johnson, D. H.; Mininberg, E.; Carbone, D. P.; Henderson, T.; Kim, E. S.; Blumenschein, G., Jr.; Lee, J. J.; Liu, D. D.; Truong, M. T.; Hong, W. K.; Tran, H.; Tsao, A.; Xie, D.; Ramies, D. A.; Mass, R.; Seshagiri, S.; Eberhard, D. A.; Kelley, S. K.; Sandler, A. Phase I/II trial evaluating the anti-vascular endothelial growth factor monoclonal antibody bevacizumab in combination with the HER-1/epidermal growth factor receptor tyrosine kinase inhibitor erlotinib for patients with recurrent non-small-cell lung cancer. *J. Clin. Oncol.* **2005**, *23*, 2544−2555.
(13) Saltz, L. B.; Lenz, H. J.; Kindler, H. L.; Hochster, H. S.; Wadler, S.; Hoff, P. M.; Kemeny, N. E.; Hollywood, E. M.; Gonen, M.; Quinones, M.; Morse, M.; Chen, H. X. Randomized phase II trial of cetuximab, bevacizumab, and irinotecan compared with cetuximab and bevacizumab alone in irinotecan-refractory colorectal cancer: the BOND-2 study. *J. Clin. Oncol.* **2007**, *25*, 4557−4561.
(14) Hurwitz, H.; Fehrenbacher, L.; Novotny, W.; Cartwright, T.; Hainsworth, J.; Heim, W.; Berlin, J.; Baron, A.; Griffing, S.; Holmgren, E.; Ferrara, N.; Fyfe, G.; Rogers, B.; Ross, R.; Kabbinavar, F. Bevacizumab plus irinotecan, fluorouracil, and leucovorin for metastatic colorectal cancer. *N. Engl. J. Med.* **2004**, *350*, 2335−2342.
(15) Tol, J.; Koopman, M.; Cats, A.; Rodenburg, C. J.; Creemers, G. J.; Schrama, J. G.; Erdkamp, F. L.; Vos, A. H.; van Groeningen, C. J.; Sinnige, H. A.; Richel, D. J.; Voest, E. E.; Dijkstra, J. R.; Vink-Borger, M. E.; Antonini, N. F.; Mol, L.; van Krieken, J. H.; Dalesio, O.; Punt, C. J. Chemotherapy, bevacizumab, and cetuximab in metastatic colorectal cancer. *N. Engl. J. Med.* **2009**, *360*, 563−572.
(16) Saltz, L.; Badarinath, S.; Dakhil, S.; Bienvenu, B.; Harker, W. G.; Birchfield, G.; Tokaz, L. K.; Barrera, D.; Conkling, P. R.; O'Rourke, M. A.; Richards, D. A.; Reidy, D.; Solit, D.; Vakiani, E.; Capanu, M.; Scales, A.; Zhan, F.; Boehm, K. A.; Asmar, L.; Cohn, A. Phase III trial of cetuximab, bevacizumab, and 5-fluorouracil/leucovorin vs. FOLFOX-bevacizumab in colorectal cancer. *Clin. Colorectal Cancer* **2011**, *11*, 101−111.
(17) Hecht, J. R.; Mitchell, E.; Chidiac, T.; Scroggin, C.; Hagenstad, C.; Spigel, D.; Marshall, J.; Cohn, A.; McCollum, D.; Stella, P.; Deeter, R.; Shahin, S.; Amado, R. G. A randomized phase IIIB trial of chemotherapy, bevacizumab, and panitumumab compared with chemotherapy and bevacizumab alone for metastatic colorectal cancer. *J. Clin. Oncol.* **2009**, *27*, 672−680.
(18) Heskamp, S.; Boerman, O. C.; Molkenboer-Kuenen, J. D. M.; Oyen, W. J. G.; van der Graaf, W. T. A.; van Laarhoven, H. W. M. Bevacizumab reduces tumor targeting of anti-epidermal growth factor and anti-insulin-like growth factor 1 receptor antibodies. *Int. J. Cancer* **2013**, *133*, 307−314.
(19) Brom, M.; Joosten, L.; Oyen, W. J.; Gotthardt, M.; Boerman, O. C. Improved labelling of DTPA- and DOTA-conjugated peptides and antibodies with ^{111}In in HEPES and MES buffer. *EJNMMI Res.* **2012**, *2*, 4.
(20) Prahallad, A.; Sun, C.; Huang, S.; Di Nicolantonio, F.; Salazar, R.; Zecchin, D.; Beijersbergen, R. L.; Bardelli, A.; Bernards, R. Unresponsiveness of colon cancer to BRAF(V600E) inhibition through feedback activation of EGFR. *Nature* **2012**, *483*, 100−103.
(21) van der Have, F.; Vastenhouw, B.; Ramakers, R. M.; Branderhorst, W.; Krah, J. O.; Ji, C.; Staelens, S. G.; Beekman, F. J. U-SPECT-II: an ultra-high-resolution device for molecular small-animal imaging. *J. Nucl. Med.* **2009**, *50*, 599−605.
(22) Span, P. N.; Grebenchtchikov, N.; Geurts-Moespot, J.; Westphal, J. R.; Lucassen, A. M.; Sweep, C. G. EORTC Receptor and Biomarker Study Group Report: a sandwich enzyme-linked immunosorbent assay for vascular endothelial growth factor in blood and tumor tissue extracts. *Int. J. Biol. Markers* **2000**, *15*, 184−191.
(23) Grebenchtchikov, N.; Sweep, C. G.; Geurts-Moespot, A.; Piffanelli, A.; Foekens, J. A.; Benraad, T. J. An ELISA avoiding interference by heterophilic antibodies in the measurement of components of the plasminogen activation system in blood. *J. Immunol. Methods* **2002**, *268*, 219−231.
(24) Grebenchtchikov, N.; Geurts-Moespot, A. J.; Heijmen, L.; Laarhoven, H. W. M.; van Herpen, C. M. L.; Thijs, A. M. J.; Span, P. N.; Sweep, F. C. G. J. Quantification of patient specific assay interference in different formats of enzyme linked immunoassays for therapeutic monoclonal antibodies. *Ther. Drug Monit.* **2014**, 10.1097/FTD.0000000000000090.
(25) Wang, Y.; Dong, L.; Bi, Q.; Li, X.; Wu, D.; Ge, X.; Zhang, X.; Fu, J.; Zhang, C.; Wang, C.; Li, S. Investigation of the efficacy of a bevacizumab−cetuximab−cisplatin regimen in treating head and neck squamous cell carcinoma in mice. *Targeted Oncol.* **2010**, *5*, 237−243.
(26) Poindessous, V.; Ouaret, D.; El Ouadrani, K.; Battistella, A.; Megalophonos, V. F.; Kamsu-Kom, N.; Petitprez, A.; Escargueil, A. E.; Boudou, P.; Dumont, S.; Cervera, P.; Flejou, J. F.; Andre, T.; Tournigand, C.; Chibaudel, B.; de Gramont, A.; Larsen, A. K. EGFR- and VEGF(R)-targeted small molecules show synergistic activity in colorectal cancer models refractory to combinations of monoclonal antibodies. *Clin. Cancer Res.* **2011**, *17*, 6522−6530.
(27) Arjaans, M.; Oude Munnink, T. H.; Oosting, S. F.; Terwisscha van Scheltinga, A. G.; Gietema, J. A.; Garbacik, E. T.; Timmer-Bosscha, H.; Lub-de Hooge, M. N.; Schroder, C. P.; de Vries, E. G. Bevacizumab-induced normalization of blood vessels in tumors hampers antibody uptake. *Cancer Res.* **2013**, *73*, 3347−3355.
(28) Pastuskovas, C. V.; Mundo, E. E.; Williams, S. P.; Nayak, T. K.; Ho, J.; Ulufatu, S.; Clark, S.; Ross, S.; Cheng, E.; Parsons-Reponte, K.; Cain, G.; Van Hoy, M.; Majidy, N.; Bheddah, S.; Dela Cruz Chuh, J.; Kozak, K. R.; Lewin-Koh, N.; Nauka, P.; Bumbaca, D.; Sliwkowski, M. X.; Tibbitts, J.; Theil, F. P.; Fielder, P. J.; Khawli, L. A.; Boswell, C. A.

Effects of anti-VEGF on pharmacokinetics, biodistribution and tumor penetration of trastuzumab in a preclinical breast cancer model. *Mol. Cancer Ther.* **2012**, *11*, 752−762.
(29) Bruns, C. J.; Harbison, M. T.; Davis, D. W.; Portera, C. A.; Tsan, R.; McConkey, D. J.; Evans, D. B.; Abbruzzese, J. L.; Hicklin, D. J.; Radinsky, R. Epidermal growth factor receptor blockade with C225 plus gemcitabine results in regression of human pancreatic carcinoma growing orthotopically in nude mice by antiangiogenic mechanisms. *Clin. Cancer Res.* **2000**, *6*, 1936−1948.
(30) Perrotte, P.; Matsumoto, T.; Inoue, K.; Kuniyasu, H.; Eve, B. Y.; Hicklin, D. J.; Radinsky, R.; Dinney, C. P. Anti-epidermal growth factor receptor antibody C225 inhibits angiogenesis in human transitional cell carcinoma growing orthotopically in nude mice. *Clin. Cancer Res.* **1999**, *5*, 257−265.
(31) Boerman, O. C.; Sharkey, R. M.; Blumenthal, R. D.; Aninipot, R. L.; Goldenberg, D. M. The presence of a concomitant bulky tumor can decrease the uptake and therapeutic efficacy of radiolabeled antibodies in small tumors. *Int. J. Cancer* **1992**, *51*, 470−475.
(32) Hagan, P. L.; Halpern, S. E.; Dillman, R. O.; Shawler, D. L.; Johnson, D. E.; Chen, A.; Krishnan, L.; Frincke, J.; Bartholomew, R. M.; David, G. S.; et al. Tumor size: effect on monoclonal antibody uptake in tumor models. *J. Nucl. Med.* **1986**, *27*, 422−427.
(33) Ellis, L. M.; Hicklin, D. J. VEGF-targeted therapy: mechanisms of anti-tumour activity. *Nat. Rev. Cancer* **2008**, *8*, 579−591.